JOURNAL OF MATERIALS SCIENCE 12 (1977) 2411–2420

Scanning electron microscope studies of local variations in cathodoluminescence in striated ZnS platelets

S. DATTA, B. G. YACOBI*, D. B. HOLT
Department of Metallurgy and Materials Science, Imperial College of Science and Technology, London, UK

The local variations in cathodoluminescence (CL) observed in structurally complex ZnS platelets, arise from structural changes, impurity segregation and internal electrical field effects. By determining local crystal structures using birefringence, the position of the peak of the "edge" (conduction to valence band) CL band was calibrated. This could then be used to determine local crystal structures with the spatial resolution of the SEM. The variation of the peak position of certain impurity bands was determined by this means as a function of crystal structure. Finally by using faulted and unfaulted regions, the effect of the intense local electric fields, due to faulting, in quenching CL (i.e. decreasing emitted intensities) was observed. The importance of correcting the raw emission spectral data for the varying response of the detection system is emphasized. Emission band heights, positions and shapes are markedly altered. Only the corrected CL emission spectra are reliable for analytical work. Spectra in "arbitrary units" and both panchromatic and monochromatic CL micrographs can be misleading.

1. Introduction

Scanning electron microscopy (SEM) spectroscopic cathodoluminescence (CL) results were first published by Williams and Yoffe using samples of striated ZnSe [1, 2] and ZnS [3, 4]. The local variations in CL emission observed were related to the crystal defect structure deduced from other experiments such as transmission electron microscopy. They showed that in cooled ZnS platelets, the edge emission band (which consists of photons having energy values near that of the forbidden gap) contained characteristic bound exciton lines which were ascribed to hexagonal or cubic phase material. Subsequently, a series of monochromatic (one wavelength) micrographs were presented by Yoffe *et al.* [5]. The effect of increasing beam current density was also discussed.

Holt and Culpan [6] used the conductive, cathodoluminescent and emissive modes of the SEM to examine ZnS platelets with striated structures. Their results indicated that not only did stacking faults and polytypic intergrowths correlate with changes in ZnS emission, but also some local variations could be due to inhomogeneous impurity distributions.

All the above literature indicates that local variations in CL emission from structurally complex ZnS platelets may be due to (i) changes in structure (ii) impurity segregation, and/or (iii) internal electric field effects. This paper reports the results of a further investigation of these effects.

2. Experimental details

A Cambridge IIA Scanning Electron Microscope fitted with an efficient spectroscopic light detection system was used for cathodoluminescence (CL) emission measurements. The electron beam was incident on the crystal at one focus of a semi-ellipsoidal mirror. A quartz fibre (Schott-u.v.) optic light guide placed near the other focus

*Present address: Department of Physics, University of Waterloo, Ontario, Canada, N2L 3G1.

© *1977 Chapman and Hall Ltd. Printed in Great Britain.*

collected all the emitted luminescence and passed it to a grating monochromator (Bentham Instruments), a cooled photomultiplier (EMI 9558QA) with an S20 response and a photon counter (SSR Instruments). The output of the photon counter, a pulse train, can be connected simultaneously to a video screen of the SEM to produce monochromatic or panchromatic CL micrographs or stored in a multichannel scaler for computer processing. To obtain the true CL emission spectra, the calibrated fraction of the photons emitted which give rise to a counted pulse in the detector, as a function of wavelength, was stored in the computer and used to correct all raw count-rate data. The CL detector system and its calibration are described in detail elsewhere [7, 8].

The striated ZnS platelets used in these experiments were all obtained from the Hebrew University of Jerusalem. They were grown by sublimation in H_2S [9, 10] and were structurally non-uniform, consisting of parallel strips of different birefringence, all perpendicular to the common *c*-axis. The various strips may have either the hexagonal structure (wurtzite), the cubic structure (sphalerite) or one of the many polytypic forms.

The spatial resolution of the SEM (a few microns) allowed small structurally homogeneous areas from the same platelet to be examined. This was essential as results soon showed gross variations to occur with small displacements over the specimen surface.

All the emission spectra were obtained by working at 30 keV with beam currents of 10^{-9} to 10^{-10} A. The spectral resolution used with these settings was about 5 nm. All measurements were made at room temperature.

3. Results and interpretation

Many structurally homogeneous hexagonal wurtzite (2H), cubic sphalerite (3C) and 4H polytype regions were chosen from over a dozen striated ZnS platelets for the investigation of local cathodoluminescence (CL). A typical platelet consisted of numerous structurally different areas which could be identified from birefringence measurements [10, 11]. Corrected room temperature values for the peak, E_p, of the CL edge emission band (arising from conduction band to valence band transitions) from the selected areas are given in Table I.

Brafman and Steinberger [11] showed that the various regions of such ZnS platelets differ from each other in the stacking sequence of the basal planes. The differences can be characterized by a single structure parameter β. This is the percentage of close-packed planes which are in a hexagonal nearest-neighbour environment. So the various bands can be classified as having a certain percentage of hexagonality β which is 100% for wurtzite (2H), 50% for polytype 4H and 0% for cubic sphalerite (3C) with the higher order polytypes falling between the values for the cubic and the 4H modifications. Furthermore they found that the absorption edge shifts in wavelength linearly with β. It seems reasonable therefore, to expect our 4H polytype CL edge emission peak to have an intermediate value between the two extreme structures (3C and 2H) in Table I. Recently Morozova *et al.* [12] reported CL edge emission data for a number of ZnS structural forms. Our values were generally in good agreement with theirs. Differences arose, since we have used a spectral correction procedure that allows for the fall in the total number of photons detected compared to the number generated at the sample, at all wavelengths between our detection limits (250 to 850 nm). It must be emphasized that a method of spectral correction is considered essential since earlier results [13] on the ZnS self-activated luminescence band showed that the band shape, peak position and related shape parameters change quite considerably with correction in general. However, in the case of the edge emission band, correction effects are small because it occurs in a wavelength range (325 to 345 nm) over which the system response factor is nearly constant.

TABLE I Cathodoluminescence edge emission peak energies for various ZnS structures at room temperature.

Crystal structure	E_p (eV)
Hexagonal (Wurtzite)	3.740 (331 nm)
4H Polytype	3.706 (335 nm)
Cubic (Sphalerite)	3.657 (339 nm)

As outlined earlier, local cathodoluminescence variations may be attributed to (i) structural changes or to (ii) impurity segregation or to (iii) internal electric field effects. It is the purpose of this paper to evaluate the relative importance of each of these contributory causes. Structural changes are easily identified from birefringence measurement as already explained. Fig. 1a shows a typical ZnS platelet (No. 227B) photographed under crossed polarizers in an optical microscope. The polytypic bands, which appear with different

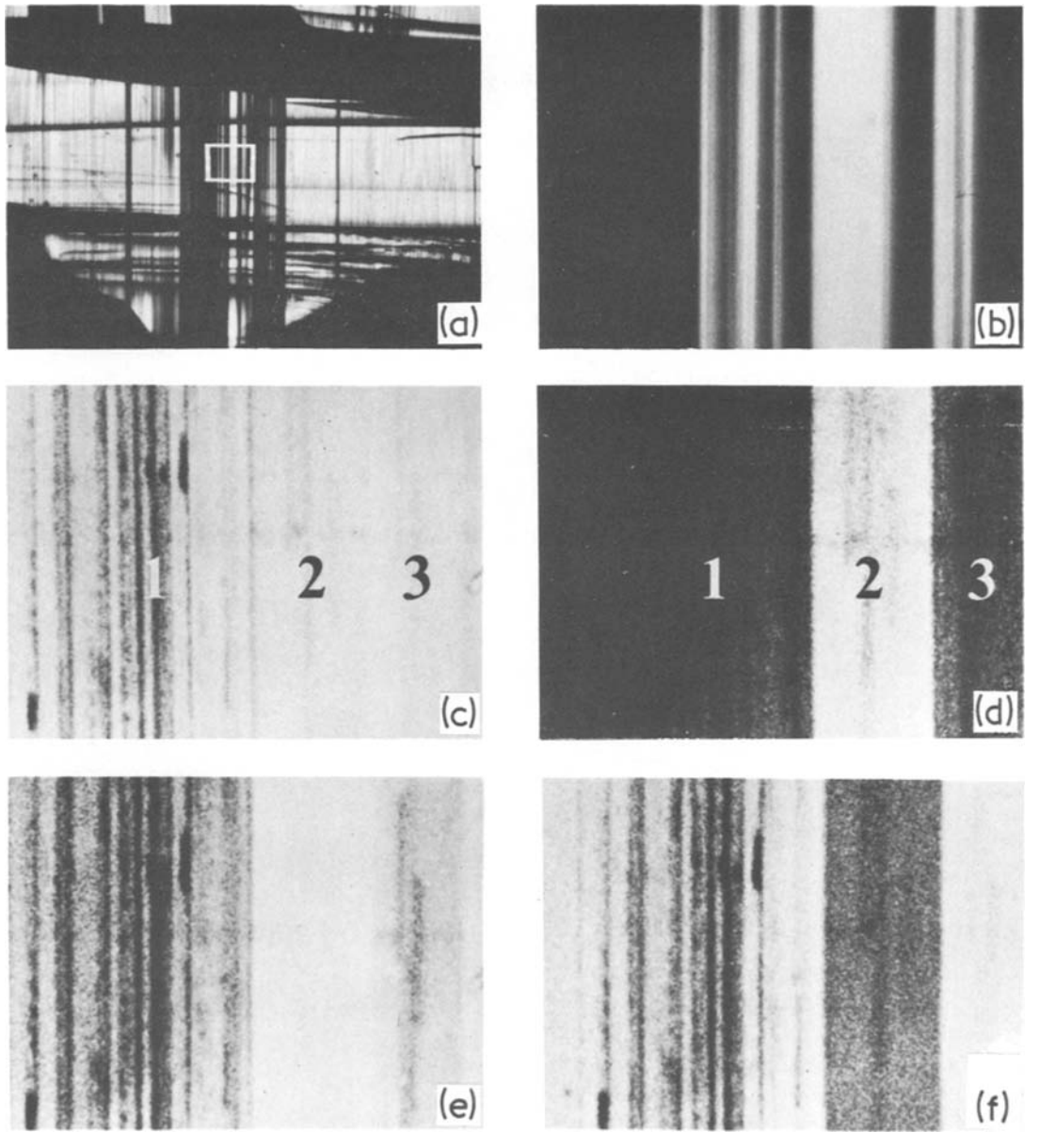

Figure 1 Micrographs of a striated ZnS (227B) platelet with the common *c*-axis running horizontally. (a) is a low magnification polarized light micrograph of the whole platelet, showing the polytypic bands running vertically. The remaining micrographs are all of the area in the rectangle outlined in the centre of the platelet. (b) is an enlargement of the area outlined in (a). (c) is a panchromatic CL SEM micrograph. The remaining pictures are monochromatic CL SEM micrographs recorded at the following emission wavelengths: (d) 328 mm (3.7 eV), (e) 334 nm (3.71 eV), and (f) 344 nm (3.60 eV). The width of the area represented by the CL micrographs (c), (d), (e) and (f) is 308 μm.

colours under these conditions, run perpendicularly to the polar *c*-axis of the crystal. The other fine lines running horizontally along the *c*-axis are called linear markings and are growth steps [14]. Regions containing them have been avoided when taking spectra. An enlargement of the delineated area, in which CL measurements were made, is given in Fig. 1b. Region 1 was a heavily faulted cubic area, region 2 a 4H polytypic band and region 3 a broad unfaulted cubic band. Due to the intrinsic nature of the edge emission, recording at wavelengths between 325 and 345 nm at room temperature probably eliminates serious impurity perturbations. However, care is needed in inter-

preting results because analysis of the shape of the edge emission band in ZnS revealed two distinctive exponential regions in the low-energy side of the band [15] and the lower of the two sectors is believed to be influenced by both impurity concentration and temperature.

The remainder of Fig. 1 is made up of panchromatic (all wavelengths) (c) and monochromatic (one wavelength) CL micrographs (d, e and f). The width of the area represented is about 308 μm. Changes between the micrographs are considerable because each structure has an unique edge peak emission value (Table I) and depending on the wavelength used as signal for the micrograph, regions appear light or dark. One feature of particular interest is region 1, where little or no emission occurs at any wavelength. This contrasts with the behaviour of the broader, second cubic region 3. By magnifying and taking spectra from one of the dark lines, in region 1 in Fig. 1f it was found to emit low-intensity cubic edge luminescence. To compare relative photon emission from the three regions, equal volumes of each type of material were examined under identical SEM conditions. The results in Fig. 2 show marked quenching (reduction) of the CL emission to occur in region 1 as compared to region 3 which has the same structure (3C). This may be attributed to internal electric field quenching. The existence of strong macroscopic internal fields, which are dependent on structure, has been thoroughly established in these ZnS platelets [16, 17]. These fields occur due to charged sheets of dislocations [18, 19], which occur whenever there is a lattice-constant misfit between adjacent crystal structures and have field strengths up to 10^5 V cm^{-1} in the more densely faulted regions of a platelet [20]. The spatial resolution of the spectroscopic CL mode of the SEM was necessary to confirm that this electric field effect was the cause of the reduced emission from region 1. Without it the CL micrographs give little evidence of the cause of the low luminosity of region 1.

Local variations in impurity-activated CL were also investigated using the same sample. Typical monochromatic CL micrographs and spectra are

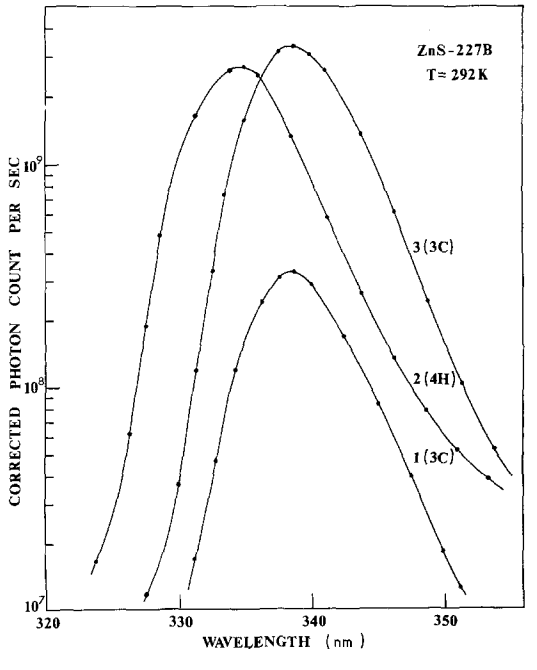

Figure 2 The CL edge band emission obtained from the three numbered regions of Fig. 1d.

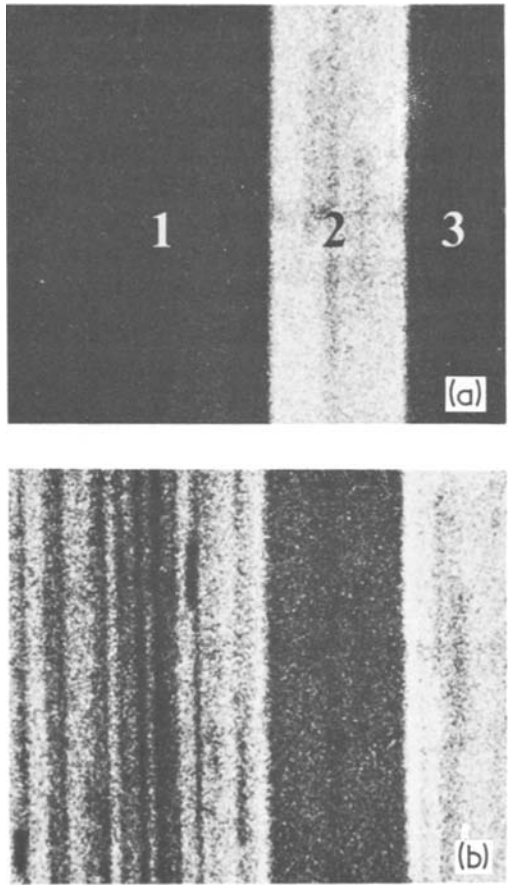

Figure 3 Monochromatic CL SEM micrographs of the same area as in Fig. 1. (a) at a wavelength of 670 nm (1.85 eV) and (b) 685 nm (1.81 eV). The width of the area represented in these two micrographs is approximately 294 μm with the polar c-axis of the crystal running horizontally.

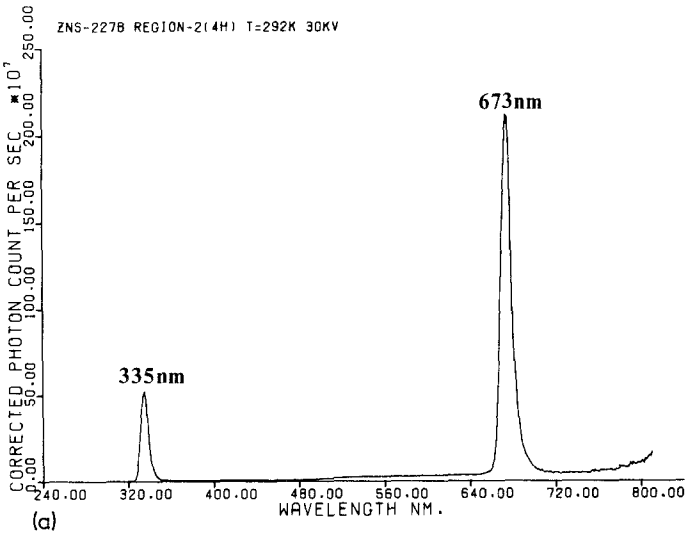

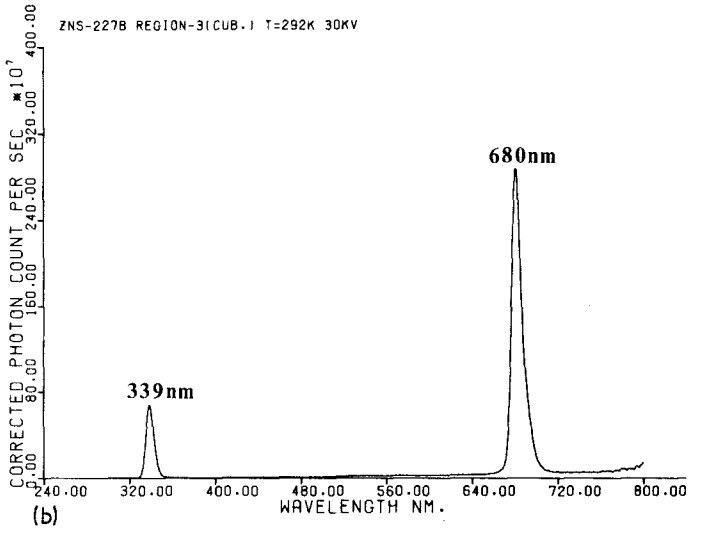

Figure 4 CL emission spectra from the areas marked in Fig. 3. (a) the spectrum from region 2 and (b) the spectrum from area 3. The shorter wavelength band is the edge emission (conduction band to valence band recombination radiation). The sharp band at longer wavelengths is due to an impurity activated mechanism.

given in Figs. 3 and 4 respectively. The spectra show that the emission consists of two relatively sharp bands well separated in wavelength (Fig. 4). The one at shorter wavelength (higher energy) is due to the edge emission (cf Fig. 2) whilst the other is an impurity band.

Although the samples studied here were of the highest purity available for ZnS they still contained many uncontrolled impurities in concentrations of the order of ppm. These varied both in type and concentration from one growth run to the next [9]. Not only were the common metallic impurities like Cu, Al, Fe and Mn found, but some of the less common impurities like Pb, Ti and Sn were also sometimes present (Spectrochemical analysis, The Weizmann Institute, Israel).

The values given in Table II for the impurity band peak energy E_i (eV) show that there is a shift towards lower energies (longer wavelengths) in going from region 2 (4H polytype) to region 3 (cubic). This behaviour taken together with the fact that the ratio of E_p (for edge emission) to E_i (for empurity emission) remains constant suggests that the same impurity is responsible for the observed red luminescence band in both structures. Thus region 2 in Fig. 3a, appears bright because this micrograph was recorded using a photon energy near the impurity band peak E_i for the 4H

TABLE II Room temperature cathodoluminescence peak energies for tin (Sn) activated ZnS (No. 227B).

Crystal structure	E_i (eV)
4H Polytype	1.842 (673 nm)
Cubic (Sphalerite)	1.823 (680 nm)

polytype but the relative brightness soon moves to region 3 in Fig. 3b, as the wavelength recorded moves towards the cubic impurity peak value. Since the impurity band gives a high rate of photon emission and is well defined, local CL contrast changes greatly over just a few intervals of the wavelength resolution of the detection system. Internal electric field quenching of region 1 was also observed for this impurity band.

By comparison of our spectral measurements with data in the luminescence literature, the impurity responsible for our red band may be identified. General reviews on the optical and luminescence properties of II–VI compounds are given by Curie and Prener [21] and Shionoya [22]. Copper [23–25] and tin [26–28] impurities have been found to produce red emission bands in ZnS which fall in the wavelength range 670 to 680 nm. There are two facts which make it appear that red-copper (R-Cu) luminescence is unlikely to be the explanation of the impurity band reported here: (a) for R-Cu emission to occur there must be no coactivation from group IIIB or VIIB elements [25], otherwise the emission occurs in another wavelength region; however, aluminium (group IIIB) is known from spectrochemical analyses to be present in our samples; (b) the usually reported half-width value for R-Cu emission at room temperature, 0.65 eV, is larger by something like an order of magnitude than that in our observations (e.g. those in Fig. 4).

It therefore seems more probable that our red band can be assigned to tin activation. In fact the peak position given by Mita [27] for tin-activated cubic ZnS agrees with those reported in Table II.

Finally, an example of preferential impurity segregation perpendicular to the *c*-axis was found in another platelet (ZnS-248). Using the data in Table I, structurally homogeneous regions were chosen by means of edge emission observations. In this way it was established that region 1 and 2 (Fig. 5) in ZnS-248 were cubic (3C) and 4H polytypic structures respectively. Birefringence measurements were later taken to check the CL structure determinations.

The panchromatic and monochromatic CL micrographs for the second sample are shown in Fig. 5a and b. Selected area spectra (uncorrected) from the two structures involved are given in Fig. 6a and c with corrected spectra in Fig. 6 b and d respectively. The impurity emission characteristics of the two areas are very different even though the

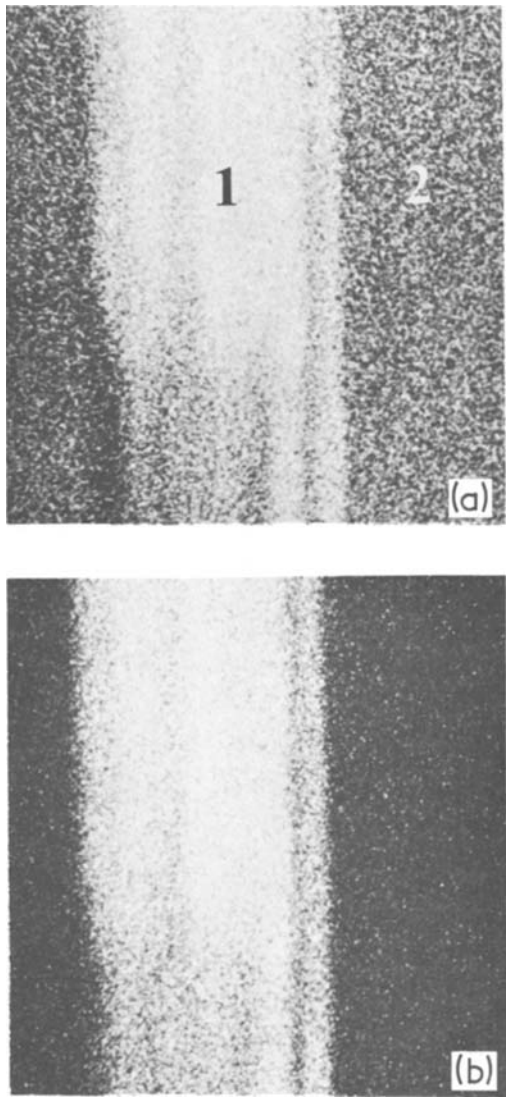

Figure 5 CL SEM micrograph of another ZnS platelet (No. 248). (a) is panchromatic and (b) is monochromatic, recorded at 523 nm (2.37 eV). The polar *c*-axis runs horizontally and the area represented is 178 μm wide.

two regions are adjacent and the spectra were taken only about 60 μm apart in the two structures. The panchromatic CL micrograph, Fig. 5a, is best described as the result of the combination of the two uncorrected spectra. The intense luminescence in region 1 (cubic) is due to the broad impurity band peaking at 523 nm (2.37 eV) (see Figs. 5b and 6a) which is missing in the adjacent 4H structure. (Fig. 5b, was recorded using the raw count rate at the uncorrected peak wavelength as video signal). Thus Fig. 5b shows that in the ZnS platelet an impurity segregated in

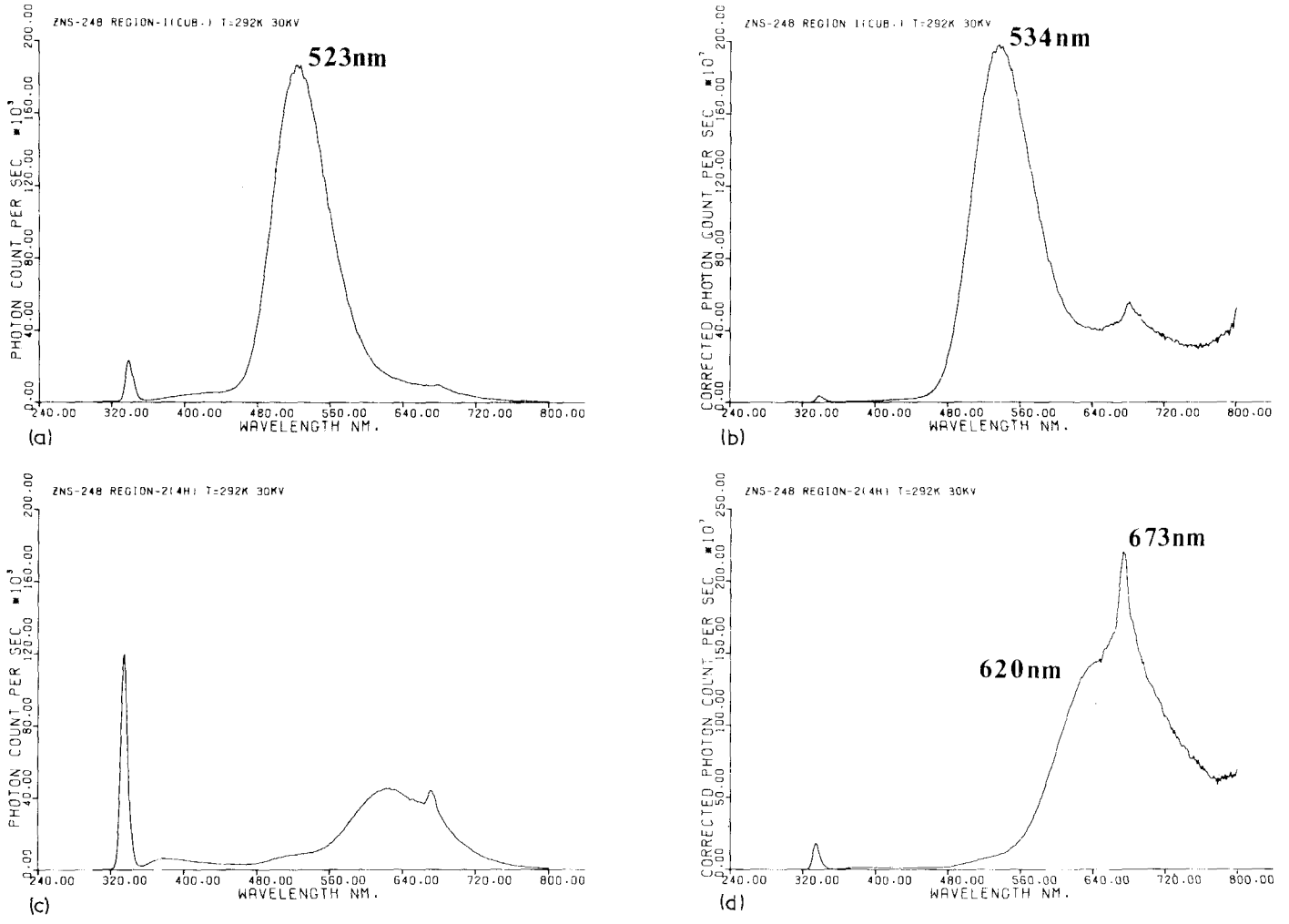

Figure 6 Uncorrected and corrected CL emission spectra obtained from the two regions shown in Fig. 5. (a) is the uncorrected spectrum from cubic region 1 and (b) is the corrected spectrum. (c) is the uncorrected spectrum from 4H polytype region 2, and (d) is that for the same region after correction. The small bands below 350 nm are the intrinsic edge emission bands while the large bands at longer wavelengths are characteristic of impurities.

the region of the crystal of one structure in preference to the other. Note, that the relative brightness of different areas in a panchromatic micrograph alone is not proof of segregation. On correction, the impurities present in the two areas are in fact found to be of equal emission strengths. This makes the panchromatic CL micrograph (Fig. 5a) unreliable as an indicator of impurity segregation since both regions should (but do not) appear as bright bands of different emission wavelengths. Equally, the monochromatic CL micrograph must be interpreted with caution. For example, Fig. 5b was taken at 523 nm (2.37 eV) which corresponds to the peak energy value of the uncorrected impurity band (Fig. 6a), whereas the corrected band maximum is at 534 nm (2.32 eV), Fig. 6b.

It is obviously possible, by using on-line computer-corrected spectral data, to obtain corrected monochromatic micrographs. This we are at present arranging but this facility was not available during the work reported here. However, it may still be necessary sometimes to work at wavelengths off the corrected peak in order that the experimental (raw) count rate gives a sufficiently high signal strength in relation to the noise in the detector-display system to obtain a good picture.

In Fig. 6a, b, c and d the edge emission is the band with the highest energy in each case. The various impurity bands were identified from their peak position and half-width values as before. The 523 nm (uncorrected, i.e. 2.37 eV) emission band in region 1 (cubic) is the well known green-copper (G-Cu) luminescence which occurs when ZnS is copper activated with aluminium as the co-activator [29–32]. Taking account of the spread in results for the G-Cu band in the literature, there is still a discrepancy between our peak value and those usually given. It appears that three factors could contribute to produce this discrepancy. Firstly, the emission results of Lorenz and Orton [33] from samples of InP, GaAs and many III–V ternary alloys, show that the CL and photoluminescence (PL) modes of excitation do not produce identical emission spectra. They found that PL produced emission bands with their peaks at greater wavelengths than did CL. Similar conclusions can be drawn from the work of Norris *et al.* [34] who used ZnS and CdS specimens. Secondly, the dependence of the green-Cu CL on the concentration of aluminium and copper was investigated by Kawai *et al.* [35]. A shift of peak wavelength was observed with increase in concentration but their results are further complicated by their use of polycrystalline samples. Thirdly, the results of our experiments have already shown that structural changes can produce large changes in the spectra for small displacements over the specimen surface. The disagreements in peak positions of the extensively studied G-Cu luminescence band reported in the luminescence literature are also probably an effect of changing the initial PL excitation wavelength [36].

The sharp impurity peak at 673 nm (1.84 eV) (Fig. 6d) from region 2 (4H polytype) in Fig. 5 is believed to be due to tin activation. This peak position agrees with the value given in Table 2 (Fig. 4a) for the earlier ZnS-227B sample. There is, in addition, a poorly resolved shoulder appearing at 620 nm (2.0 eV), the identity of which is unknown.

4. General discussion

4.1. Spectral correction

There is a rapid fall in the CL detector response curve in going from the blue (shorter wavelength) to the red (longer wavelength) end of the visible spectrum. This is mainly due to the steep fall in the quantum efficiency of S20 type (trialkali photocathode) photomultipliers over this range [8].

Broad emission bands undergo larger correction effects than do narrower bands [13]. An example seen in this work is the G-Cu emission (Fig. 6a) for which the uncorrected peak maximum appears at 523 nm (2.37 eV) but the real emission peak is found at 534 nm (2.32 eV) on correction (Fig. 6b). On the other hand, the sharp red-tin band (Fig. 6d) only shifts by approximately 1.5 nm to 673 nm (1.84 eV) on correction, although it occurs in a wavelength range where the detector response is falling rapidly.

The rate of photon emission (corrected) can be many orders of magnitude greater than the (uncorrected) raw count rate. The effects of correction on peak shape as well as position can be large. Consequently the use of absolute (corrected) spectra rather than the commonly used "arbitrary units" (uncorrected photomultiplier current or count rate) spectra is vital. Failure to correct spectra is still widespread in the luminescence literature and could account for many of the quantitative discrepancies so often reported. It

may well be that much of the irreproducibility in the literature is not entirely a consequence of uncontrolled variability in the luminescent properties of the materials studied, but at least partly due to the uncorrected use of detector systems, especially photomultipliers, of different response characteristics. Luminescence may not be as irreproducible as it appears.

Corrected emission spectra, in numbers of photons, are obviously simply related to the numbers of current pulses obtained from the photomultiplier. The number of photons emitted however is not an energy unit, although it is readily converted by multiplying by $h\nu$, the energy per photon. Conversion to candelas or lumens is also possible, but the number of photons emitted is the more useful quantity, from the fundamental point of view, since it is more easily related to the luminescent quantum efficiency and so on.

4.2. The power of the CL SEM technique

The potency of the technique arises from several factors. Firstly, the spatial resolution (from one to a few μm depending on the luminescent efficiency of the material and on the beam current and voltage consequently required) is sufficient to separate the effects of phase changes or impurity segregation. Secondly the spectral resolution and the range of wavelengths that can be detected covers both structure-dependent bands, e.g. the edge band, and impurity-dependent bands. Thirdly, corrected spectra are reproducible and, at least in principle, theoretically interpretable.

It might be thought that monochromatic CL micrographs recorded using an impurity-activated wavelength as signal could be at least semi-quantitatively interpreted as displays of the concentration of the impurity varying from point to point, as they are in the case of electron probe microanalysis micrographs. This is not possible in general because the height of the peak is not the only thing that changes from place to place. The position of the peak E_i in general shifts with changes in the crystal structure and with changes in concentration of the impurity. Two regions with the same concentration of the same impurity can therefore appear as bright and dark due to the peak occurring at the recorded wavelength in one region and right away from it in the other, as for example for the Sn peak in Fig. 3, due to a change in structure. Alternatively two regions with very different concentrations of the same impurity could appear equally bright due to a change in peak height being compensated by a shift of the peak relative to the recorded wavelength.

The only way to arrive at a reliable interpretation is to obtain the corrected "absolute" CL emission spectrum and interpret the information it contains as a preliminary to the recording for analytical purposes of any CL micrographs. An iterative procedure may in some cases be necessary, using the first micrographs to select significant areas for spectral "point" analyses followed by the recording of further micrographs. This can be continued until all the features of interest are accounted for.

5. Conclusions

(1) The cathodoluminescence (CL) edge emission peak values, E_p, at room temperature, for hexagonal (wurtzite), cubic (sphalerite) and 4H polytypic structures of ZnS are given in Table I.

(2) The results show that certain local CL variations in striated ZnS platelets can be shown to be the effects specifically of (i) structural changes, or (ii) impurity segregation, or (iii) internal electric fields.

(3) Panchromatic CL micrographs, monochromatic CL micrographs and uncorrected spectra must all be interpreted with caution since they can be misleading. Only corrected spectra give the real CL emission properties of local regions of a sample.

Acknowledgements

We are particularly grateful to P. L. Giles for his advice and support throughout this work. Financial support has been provided by the Science Research Council.

References

1. P. M. WILLIAMS and A. D. YOFFE, *Phil. Mag.* **18** (1968) 555.
2. *Idem, Nature* **221** (1969) 952.
3. *Idem, Radiation Effects* **1** (1969) 61.
4. *Idem,* in "Radiation Effects in Semiconductors", edited by J. W. Corbett and G. D. Watkins (Gordon and Breach, New York, 1971) p. 399.
5. A. D. YOFFE, K. J. HOWLETT and P. M. WILLIAMS, in Proceedings of the VIth Annual SEM Symposium (IITRI, Chicago, 1973) p. 301.
6. D. B. HOLT and M. CULPAN, *J. Mater. Sci.* **5** (1970) 546.
7. P. L. GILES, *J. Microscopie Biol. Cell.* **22** (1975) 357.
8. J. B. STEYN, P. L. GILES and D. B. HOLT, *J. Microscopy* **107** (1976) 107.

9. O. BRAFMAN, E. ALEXANDER, B. S. FRAENKEL, Z. H. KALMAN and I. T. STEINBERGER, *J. Appl. Phys.* **35** (1964) 1855.
10. E. ALEXANDER, Z. H. KALMAN, S. MARDIX and I. T. STEINBERGER, *Phil. Mag.* **21** (1970) 1237.
11. O. BRAFMAN and I. T. STEINBERGER, *Phys. Rev.* **143** (1966) 501.
12. N. K. MOROZOVA, L. V. GAMOSOV and E. E. LAKIN, *Opt. Spektrosk.* **37** (1974) 1116.
13. S. DATTA, B. G. YACOBI and D. B. HOLT, to be published.
14. S. MARDIX, Z. H. KALMAN and I. T. STEINBERGER, *Acta Cryst.* **A24** (1968) 464.
15. B. G. YACOBI, S. DATTA and D. B. HOLT, *Phil. Mag.* **35** (1977) 145.
16. G. SHACHAR, Y. BRADA, E. ALEXANDER and Y. YACOBI, *J. Appl. Phys.* **41** (1970) 723.
17. Y. BRADA, I. T. STEINBERGER and B. STONE, *Phys. Letters* **A38** (1972) 263.
18. S. MARDIX and I. T. STEINBERGER, *J. Appl. Phys.* **41** (1970) 5339.
19. I. T. STEINBERGER, E. ALEXANDER, Y. BRADA, Z. H. KALMAN, I. KIFLAWI and S. MARDIX, *J. Cryst. Growth* **13/14** (1972) 285.
20. B. G. YACOBI and Y. BRADA, *Phys. Rev.* **B10** (1974) 665.
21. D. CURIE and J. S. PRENER, in "Physics and Chemistry of II–VI Compounds", edited by M. Aven and J. S. Prener (North-Holland, Amsterdam, 1967) p. 433.
22. S. SHIONOYA, in "Proceedings of the International Conference on II–VI Semiconducting Compounds, Providence, USA", edited by D. G. Thomas (Benjamin Inc., New York, 1970) p. 1.
23. M. H. AVEN and R. M. POTTER, *J. Electrochem. Soc.* **105** (1958) 134.
24. S. SHIONOYA, T. KODA, K. ERA and H. FUJIWARA, *J. Phys. Soc. Japan. Supplement II* **18** (1963) 299.
25. S. SHIONOYA, K. URABE, T. KODA, K. ERA and H. FUJIWARA, *J. Phys. Chem. Solids* **27** (1966) 865.
26. Y. MITA, *J. Phys. Soc. Japan* **20** (1965) 1822.
27. *Idem, Japan. J. Appl. Phys.* **3** (1964) 366.
28. K. SUGIBUCHI, *Phys. Rev.* **153** (1967) 404.
29. W. VAN GOOL and A. P. CLEIREN, *Phillips Res. Repts.* **15** (1960) 238.
30. S. SHIONOYA, T. KODA, K. ERA and H. FUJIWARA, *J. Phys. Soc. Japan.* **19** (1964) 1157.
31. S. SHIONOYA, Y. KOBAYASHI and T. KODA, *J. Phys. Soc. Japan* **20** (1965) 2046.
32. S. SHIONOYA, K. ERA and Y. WASHIZAWA, *J. Phys. Soc. Japan* **21** (1966) 1624.
33. M. R. LORENZ and A. ONTON, in "Proceedings of the 10th International Conference on the Physics of Semiconductors, Cambridge, Mass. USA" (IBM Watson Research Centre, 1970) p. 444.
34. C. B. NORRIS, C. E. BARNES and W. BEEZHOLD, *J. Appl. Phys.* **44** (1973) 3209.
35. H. KAWAI, S. KUBONIWA and T. HOSHINA, *Japan J. Appl. Phys.* **13** (1974) 1593.
36. R. GRASSER. G. ROTH and A. SCHARMANN, *Z. Phys.* **249** (1971) 91.

Received 20 December 1976 and accepted 8 February 1977.